



Local ramp metering with distant downstream bottlenecks: A comparative study



Yuheng Kan^a, Yibing Wang^{a,*}, Markos Papageorgiou^b, Ioannis Papamichail^b

^a College of Civil Engineering and Architecture, Zhejiang University, PR China

^b Department of Production Engineering & Management, Technical University of Crete, Greece

ARTICLE INFO

Article history:

Received 26 April 2015

Received in revised form 9 July 2015

Accepted 26 August 2015

Available online 26 September 2015

Keywords:

Local ramp metering

Distant downstream bottlenecks

Time delay

ALINEA

PI-ALINEA

ABSTRACT

The well-known feedback ramp metering algorithm ALINEA can be applied for local ramp metering or included as a key component in a coordinated ramp metering system. ALINEA uses real-time occupancy measurements from the ramp flow merging area that may be at most a few hundred meters downstream of the metered on-ramp nose. In many practical cases, however, bottlenecks with smaller capacities than the merging area may exist further downstream, which suggests using measurements from those downstream bottlenecks. Recent theoretical and simulation studies indicate that ALINEA may lead to poorly damped closed-loop behavior in this case, but PI-ALINEA, a suitable Proportional-Integral (PI) extension of ALINEA, can lead to satisfactory control performance. This paper addresses the same local ramp-metering problem in the presence of far-downstream bottlenecks, with a particular focus on the employment of PI-ALINEA to tackle three distinct cases of bottleneck that may often be encountered in practice: (1) an uphill case; (2) a lane-drop case; and (3) an un-controlled downstream on-ramp case. Extensive simulation studies are conducted on the basis of a macroscopic traffic flow model to show that ALINEA is not capable of carrying out ramp metering in these bottleneck cases, while PI-ALINEA operates satisfactorily in all cases. A field application example of PI-ALINEA is also reported with regard to a real case of far downstream bottlenecks. With its control parameters appropriately tuned beforehand, PI-ALINEA is found to be universally applicable, with little fine-tuning required for field applications.

© 2015 Elsevier Ltd. All rights reserved.

1. Introduction

Ramp metering is a major means for freeway traffic control (Papageorgiou and Kotsialos, 2002; Bhouri et al., 2013; Frejo and Camacho, 2012; Geroliminis et al., 2011; Gomes and Horowitz, 2006; Hegyi et al., 2005; Li et al., 2014a,b; Lu et al., 2011; Meng and Khoo, 2010). The significance of ramp metering has been demonstrated in many field applications in the past three decades (Papageorgiou and Kotsialos, 2002; Bhouri et al., 2013). ALINEA is a popular and efficient local ramp metering strategy, developed on the basis of feedback control theory (Papageorgiou and Kotsialos, 2002; Papageorgiou et al., 1991; Wang et al., 2014). Since its design philosophy was developed in the late 1980s (Papageorgiou et al., 1991), ALINEA has been successfully applied to hundreds of freeway sites worldwide (Papageorgiou and Kotsialos, 2002). Despite its local operation

* Corresponding author.

E-mail address: wangyibing@zju.edu.cn (Y. Wang).

As a follow-up, this paper aims to explore extensively, via simulation studies, the ramp metering capability of PI-ALINEA with respect to a variety of distant downstream bottlenecks, as well as the sensitivity of PI-ALINEA to the distance of the bottleneck from the metered on-ramp. The paper is organized as follows. Section 2 reviews the ALINEA and PI-ALINEA strategies. Section 3 introduces the simulation model and setup. The ALINEA and PI-ALINEA performances are examined in Section 4. Section 5 presents a field application example of PI-ALINEA. The main conclusions are given in Section 6.

2. ALINEA and PI-ALINEA

ALINEA (Papageorgiou and Kotsialos, 2002; Bhouiri et al., 2013; Frejo and Camacho, 2012) aims to prevent merging congestion and maximize flow throughput in the merging area. Based on the fundamental diagram, this can be achieved by maintaining traffic occupancy o_{out} (or density ρ_{out}) in the merging area (or shortly downstream of the merging area, see (Bhouiri et al., 2013; Frejo and Camacho, 2012), around the critical occupancy o_{cr} (or the critical density ρ_{cr}) so as to maximize the mainstream flow q_{out} (Fig. 1). For this purpose, ALINEA is designed to be:

$$r(k) = r(k - 1) + K_R[\hat{o} - o_{out}(k)], \tag{1}$$

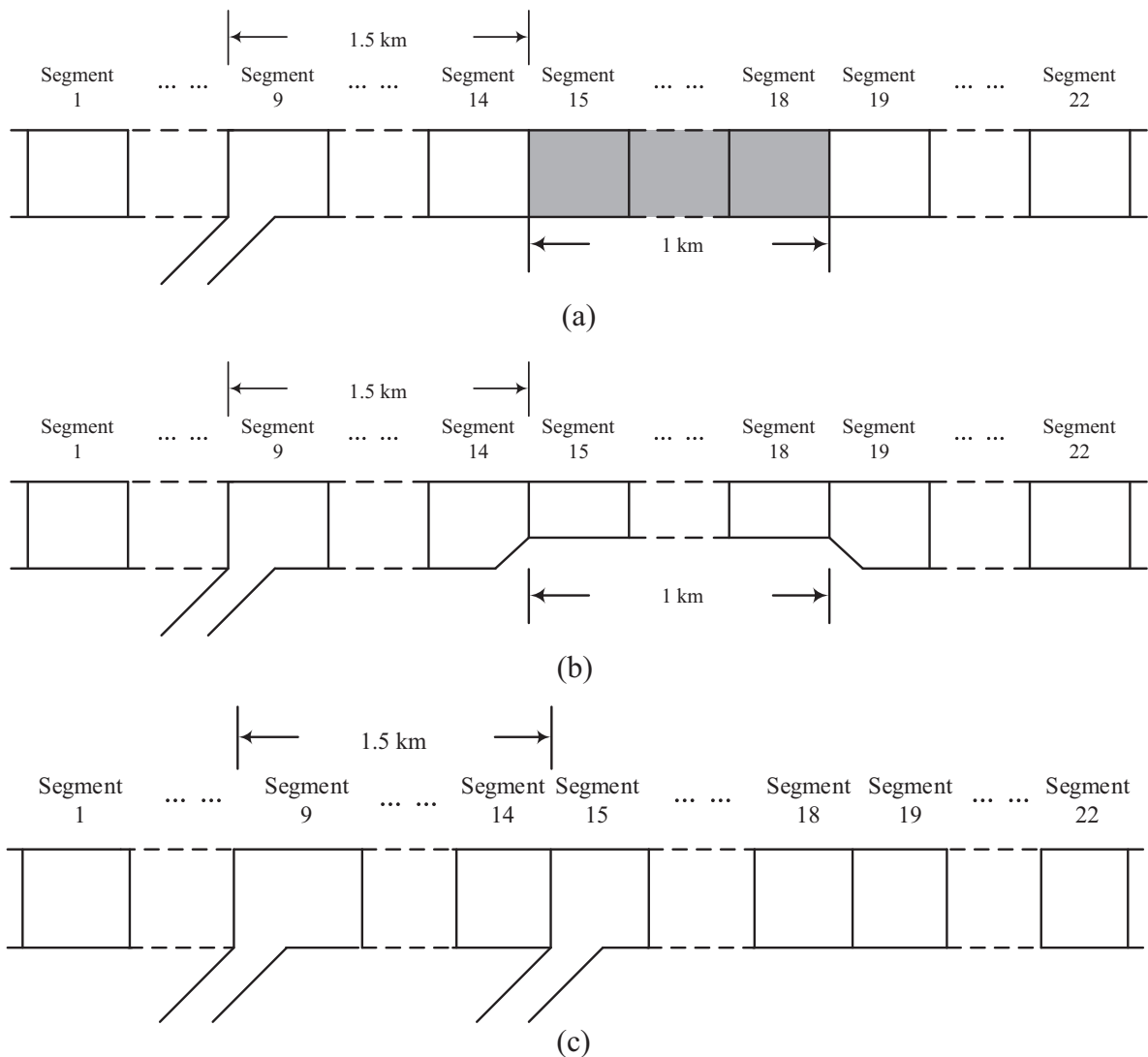


Fig. 3. A freeway stretch with a downstream bottleneck: (a) an uphill or tunnel case (Bottleneck Case 1); (b) a lane-drop case (Bottleneck Case 2); (c) an un-controlled downstream on-ramp case (Bottleneck Case 3).

where k is the discrete time index; $o_{\text{out}}(k)$ denotes lane-averaged mainstream occupancy measurements collected during the control time interval $((k-1)T, kT]$; T is within the range 20–60 s; $r(k)$ represents the on-ramp inflow applied over $[kT, (k+1)T)$; \hat{o} is a set (desired) value for the occupancy and, to the end of flow maximization, typically selected to equal o_{cr} ; $K_R > 0$ is a regulator parameter. Note also that a similar value of K_R has been successfully used in all known simulation or field applications of ALINEA, without any need for fine-tuning (Papageorgiou and Kotsialos, 2002; Papageorgiou et al., 1991; Wang et al., 2014; Papamichail and Papageorgiou, 2008). $r(k)$, determined with (1), is truncated if it exceeds a range $[r_{\text{min}}, r_{\text{max}}(k)]$. An interested reader is referred to the above references for the design principle of (1) and more details of ALINEA.

By its design philosophy, ALINEA operates with occupancy measurements collected at most a few hundred meters downstream of the metered on-ramp. If, however, a bottleneck with lower capacity than the merging area is present further downstream, the used occupancy measurements should be collected at the bottleneck. It has been shown in Wang et al. (2014) with in-depth theoretical analysis and some preliminary simulation studies that ALINEA is not efficient in maintaining the maximum throughput at the distant downstream bottleneck, while PI-ALINEA, with an extended structure:

$$r(k) = r(k-1) - K_P[o_{\text{out}}(k) - o_{\text{out}}(k-1)] + K_R[\hat{o} - o_{\text{out}}(k)], \quad (2)$$

can do a good job in both cases of a merging bottleneck and a far downstream bottleneck. Moreover, ALINEA with its K_R parameter set equal to 40 km-lane/h operates efficiently in the case of no downstream bottleneck, while PI-ALINEA, with its K_R and K_P parameters set equal to 4 km-lane/h and 100 km-lane/h, respectively, performs satisfactorily, regardless of the distance of the merging or farther downstream bottleneck from the metered on-ramp (Wang et al., 2014). That is, these parameters were found generally applicable, and not sensitive to the location of the downstream bottleneck concerned. The remainder of the paper intends to further materialize the above conclusions via extensive simulation studies.

3. Simulation model and setup

3.1. Simulation model

The utilized macroscopic traffic flow model is briefly introduced, and the interested reader is referred to (Wang et al., 2014; Papageorgiou et al., 1990; Wang and Papageorgiou, 2005) for details. The model emulates traffic hydrodynamics along a freeway stretch by use of appropriate aggregate traffic flow variables. Any considered freeway stretch is sub-divided into a number of segments and the time is discretized with a model time step (around 5–10 s). The aggregated traffic flow variables such as flow, density, and mean speed are then defined for each segment and updated for each model time step. The model involves for each segment the transport equation, conservation equation, and dynamic speed equation. The last one includes the fundamental diagram as a key component. Two fundamental diagrams FD 1 and FD 2 displayed in Fig. 2 are used in the simulation study. As shown, the free-flow speeds v_{f1} and v_{f2} are determined with the slope of the tangent of the $Q(\rho)$ -curve

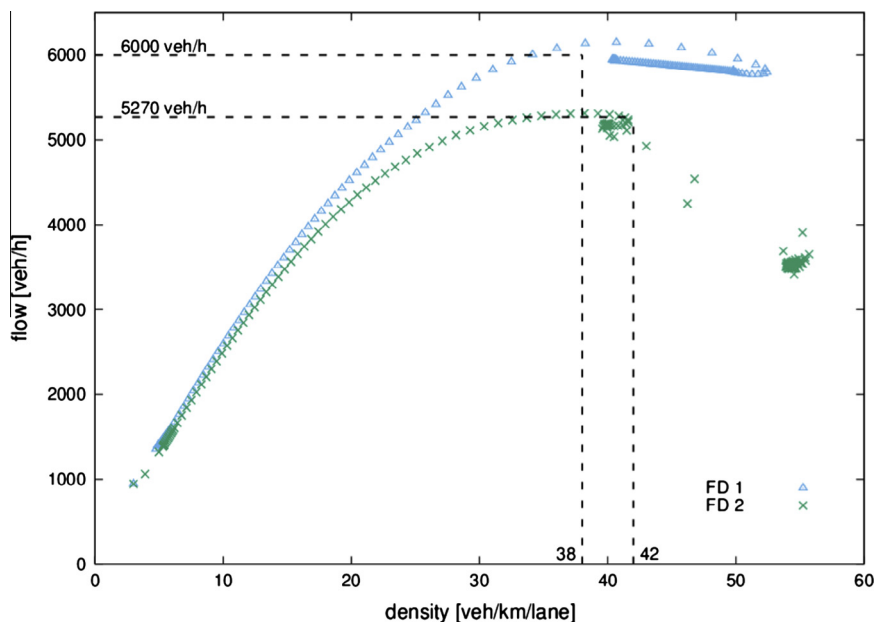


Fig. 4. The factual fundamental diagrams of segments 9 and 15 in Bottleneck Case 1.

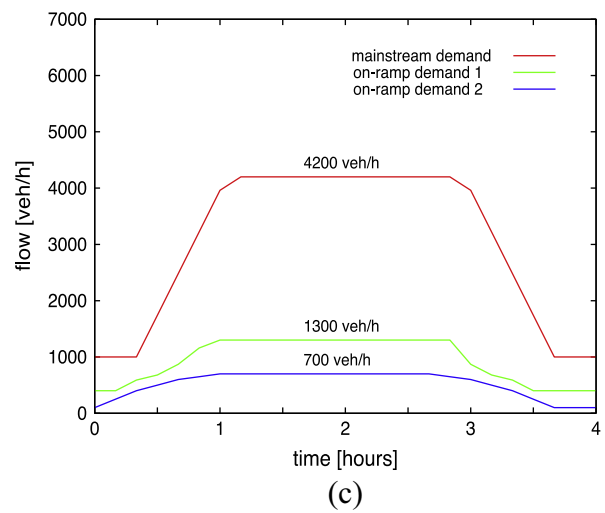
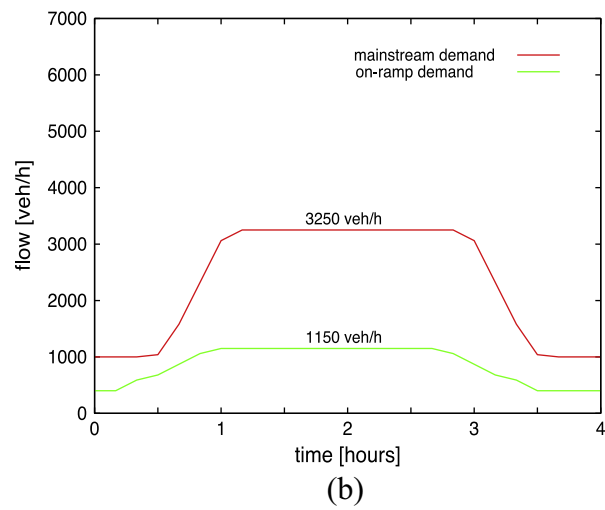
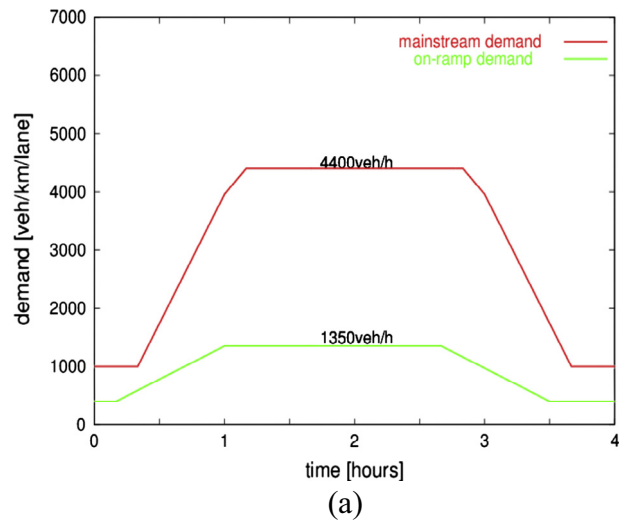


Fig. 5. The utilized demand scenarios: (a)/(b)/(c) for Bottleneck Case 1/2/3.

at $\rho = 0$; the capacities q_{cap1} and q_{cap2} are the attainable maximum flow (per lane) achieved at the critical density ρ_{cr} . Occupancy is directly related to traffic density. For the sake of simplicity, our simulation model uses density as a key variable instead. Accordingly, density is considered in (1) and (2) in place of occupancy. The simulation or model time step T_s and control time step T are 5 s and 30 s, respectively, while the minimum admissible ramp flow r_{min} and the ramp's flow capacity r_{MAX} are set equal to 300 veh/h and 2000 veh/h, respectively.

3.2. Simulation setup

3.2.1. Three cases of bottleneck

As displayed in Fig. 3, this study focuses a freeway stretch that contains a bottleneck at the far downstream of a metered on-ramp. The freeway stretches is of 5.5 km in length. Only the eastbound traffic is considered and the on-ramp is located 2 km from the start of the stretch, the bottleneck is 1 km long and located 1.5 km downstream of the on-ramp. Three cases of bottleneck are considered. In the first case (Fig. 3a) a bottleneck is present due to e.g. an uphill or curved road section or a tunnel, where lower capacity per lane is the cause for the bottleneck. The second case (Fig. 3b) is concerned with a lane-drop

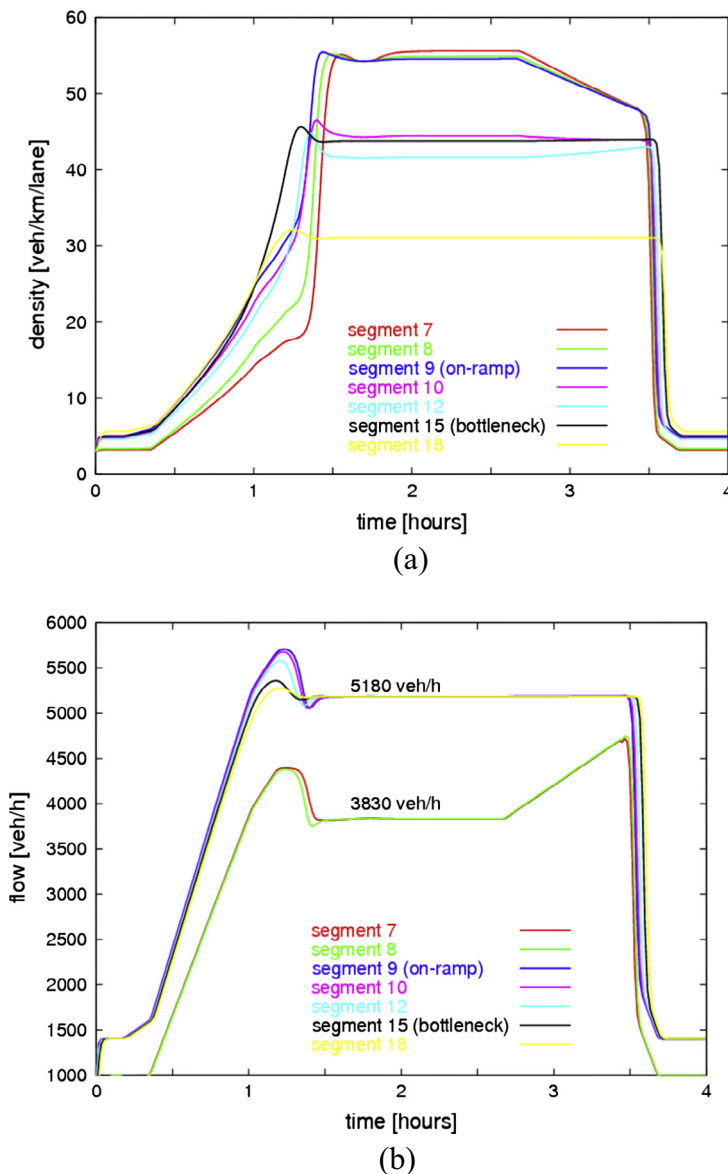


Fig. 6. No control (Bottleneck Case 1, location 1 (“Location 1” in the captions of Figs. 6–14 refers to Fig. 15a.)); (a) segment densities; (b) segment flows.

section of road, whereby the reduced capacity is due to less number of (equal-capacity) lanes. The third case (Fig. 3c) emulates the circumstance that another (un-controlled) on-ramp is situated at the far downstream of the first on-ramp; thus, the bottleneck is due to uncontrolled inflow rather than infrastructure change as in the two previous cases. Except for Case 2, the freeway stretch has three lanes throughout.

Setting the segment length equal to 0.25 km, each stretch is subdivided into 22 segments, with the (upstream/first) on-ramp located in segment 9 and the bottleneck starting in segment 15. In Case 1, the bottleneck section differs from a non-bottleneck section in traffic flow characteristics. More specifically, the fundamental diagram FD 1 (Fig. 2) is included in the simulation model to emulate each non-bottleneck segment, while FD 2 is considered for each bottleneck segment. Moreover, $\rho_{cr} = 31.4$ veh/km/lane, $v_{f1} = 105$ km/h, $v_{f2} = 79$ km/h, $q_{cap1} = 2000$ veh/h/lane, $q_{cap2} = 1500$ veh/h/lane. On the other hand, all segments in Cases 2 and 3 are characterized by FD1 only. It is only for simplicity to assume that FD 1 and FD 2 are with the same critical density (Fig. 2), but this is not essential for the pursued simulation study.

3.2.2. Factual critical densities and capacities

Due to the complex nonlinear dynamics of the utilized second-order macroscopic simulation model (Wang et al., 2014; Papageorgiou et al., 1990; Wang and Papageorgiou, 2005), the factual critical densities and capacities in each

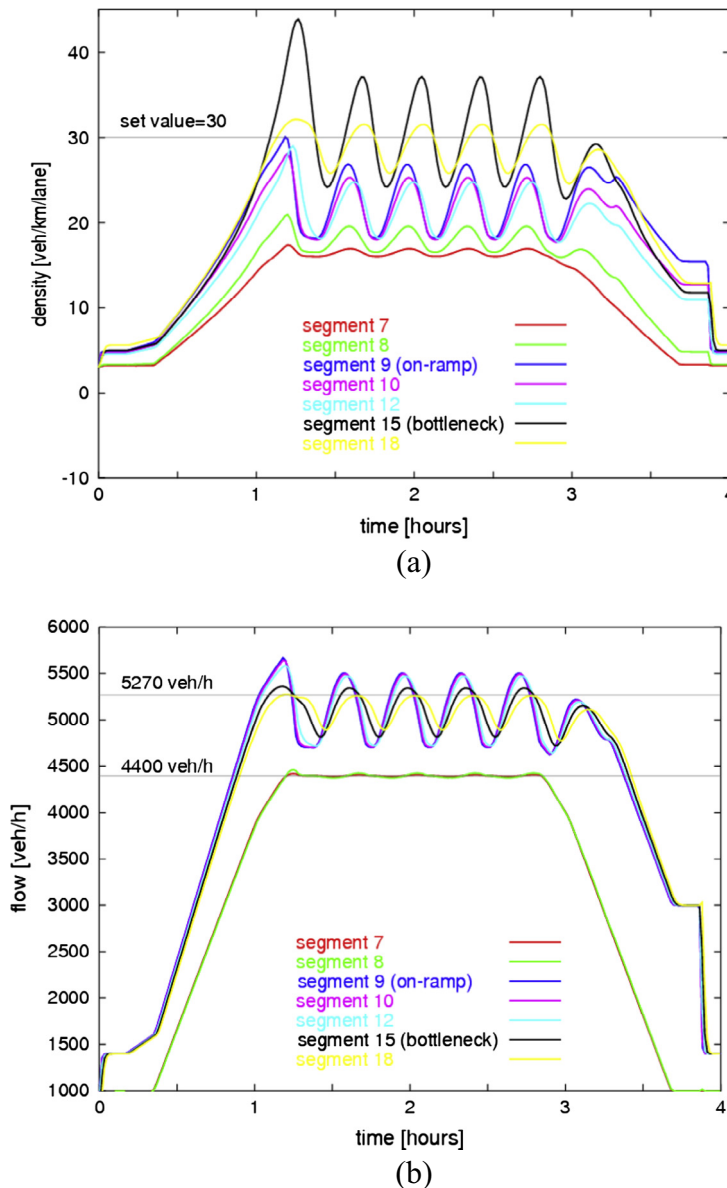


Fig. 7. ALINEA (Bottleneck Case 1, location 1): (a) segment densities; (b) segment flows.

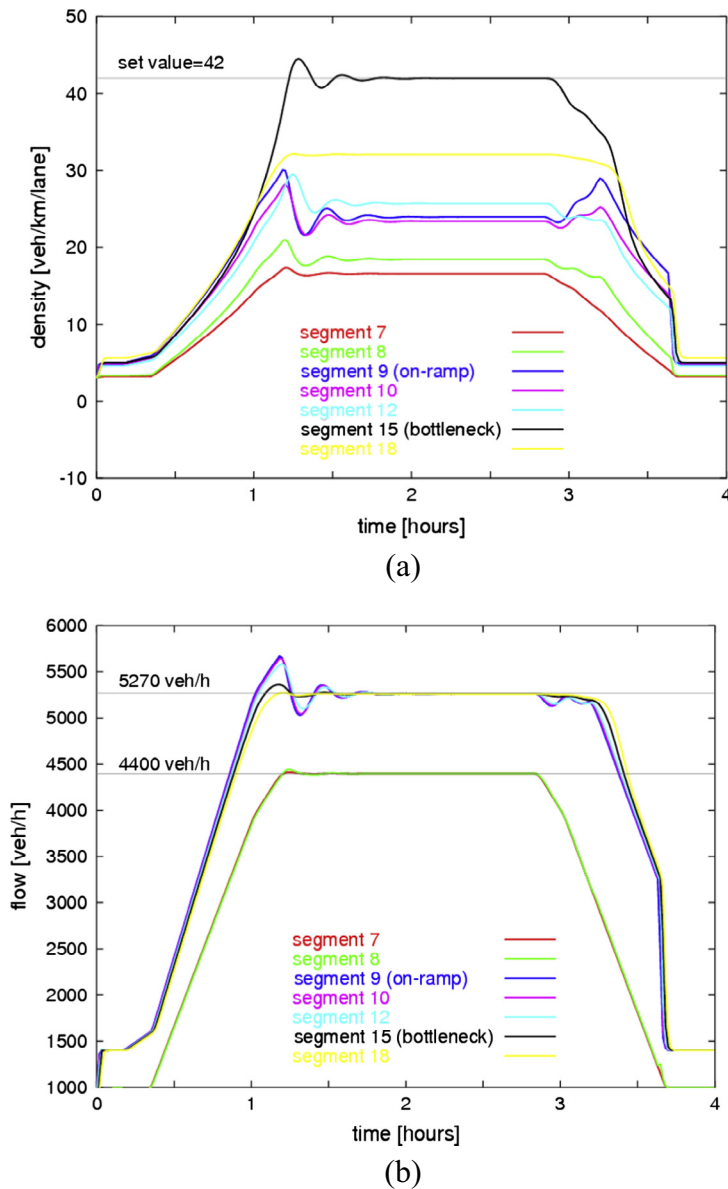


Fig. 8. PI-ALINEA (Bottleneck Case 1, location 1): (a) segment densities; (b) segment flows.

segment are not fully determined by the considered fundamental diagram functions that are only part of the model. In other words, the factual critical densities and capacities do not equal the critical densities and capacities of the given fundamental diagrams. Interested readers are referred to (Wang et al., 2014) for the exact mathematical expression of the model. To determine the factual critical densities and capacities, we did exhaustive simulation checking and figured out that the critical density for any no-bottleneck segment is around 38 veh/km/lane (rather than 31.4 veh/km/lane as given in Fig. 2), while the total capacity for 3 lanes is indeed around 6000 veh/h (as indicated by FD1). The corresponding density and total capacity values for the bottlenecks (Fig. 3) are 42 veh/km/lane and 5270 veh/h (Case 1), 41 veh/km/lane and 4300 veh/h (Case 2), and 38 veh/km/lane and 5980 veh/h (Case 3), respectively¹. Fig. 4 displays the factual fundamental diagrams based on the simulation data (for segments 9 and 15 in Case 1).² Considering the creation mechanism

¹ These specific values are dependent on the mathematical structure of the macroscopic model used as well as model parameters given (including the fundamental diagram parameters). Moreover, the mechanism of creating bottlenecks and the bottleneck locations are probably relevant too. However, these values are independent of the demand profiles considered and ramp metering algorithms applied.

² It is only for simplicity that FD1 and FD2 are assumed in the simulation model to be with the same critical density (Fig. 2). Different critical density values can be considered as well, but this has no impact on the general conclusions reached in this paper. In fact, even with the same critical density value for FD1 and FD2, the factual critical densities of the regular and bottleneck segments are not identical, as shown in Fig. 4.

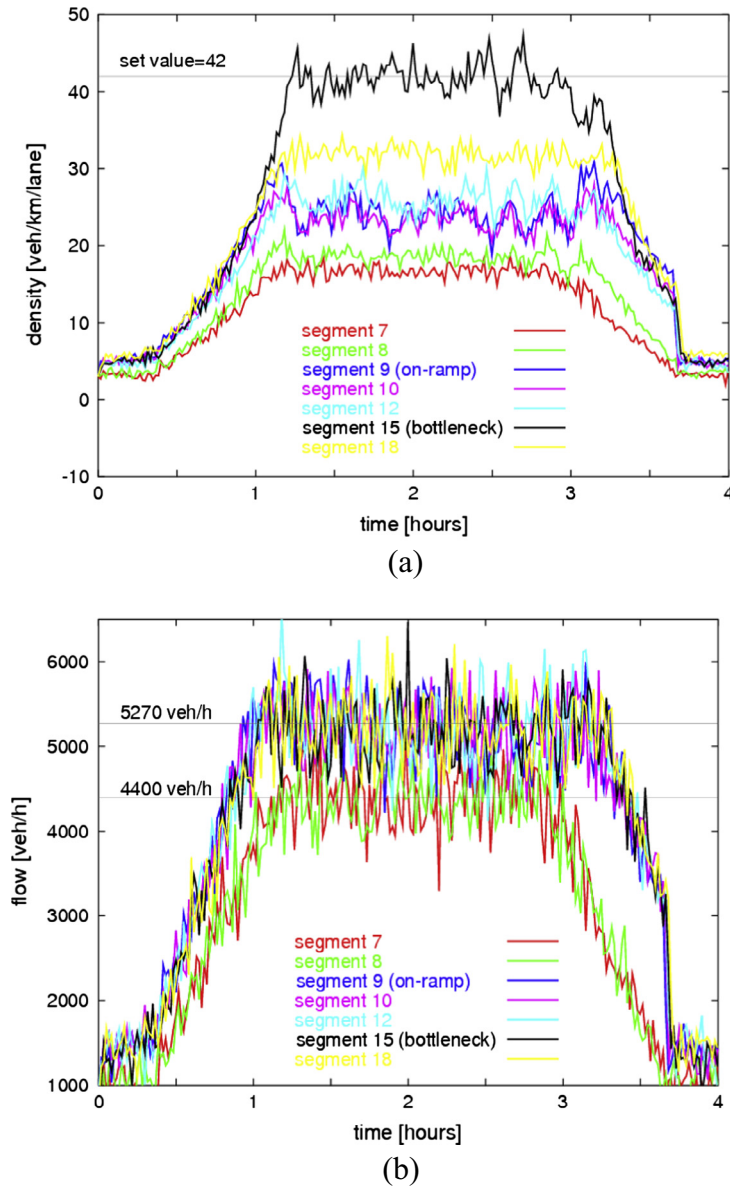


Fig. 9. PI-ALINEA (Bottleneck Case 1, location 1, stochastic): (a) segment densities; (b) segment flows.

of Case 3, it is not surprising that the factual critical density and capacity are found to be the same as those in the case of no bottleneck.

3.2.3. Demand scenarios

Some principles are based to design trapezoidal demand scenarios for the study:

- (1) The mainstream demand (at the upstream of any on-ramp) during the peak period is sufficiently lower than the capacity of any considered downstream bottleneck (else there is no role for ramp metering).
- (2) The sum of the mainstream demand and (the first) on-ramp demand is higher than the bottleneck capacity (else there is no necessity for ramp metering at the on-ramp).
- (3) The sum of the mainstream demand and (the first) on-ramp demand should be lower than the merging area capacity so that congestion (if any) appears first at the downstream bottleneck.

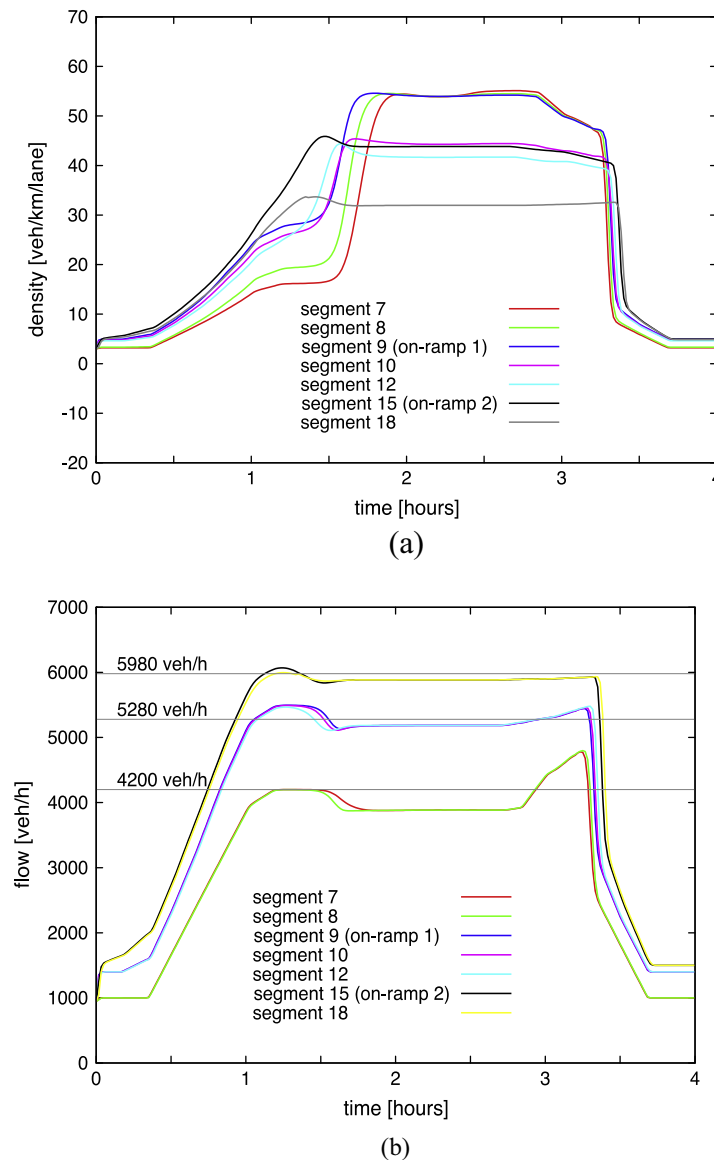


Fig. 10. No control (Bottleneck Case 3, location 1): (a) segment densities; (b) segment flows.

Following these principles, specifically for Case 3, the sum of the upstream demand and the first on-ramp demand and the sum of the upstream demand and the second on-ramp demand are both lower than the mainstream capacity, but the total demand reaching the merging area of the second on-ramp should be higher than the mainstream capacity. The specific demand profiles designed following these principles are displayed in Fig. 5.

4. Simulation investigations

Three configurations of the ramp-metering controller are considered for each bottleneck case: no ramp metering, ramp metering with ALINEA, and ramp metering with PI-ALINEA (hereafter referred to as “no control”, “ALINEA”, and “PI-ALINEA”). In this section comparative studies are conducted to demonstrate ALINEA and PI-ALINEA performance in various circumstances. Bottleneck Case 1 is considered, for which the simulation results are presented in the sequence of “no control”, “ALINEA”, and “PI-ALINEA”. Then, Cases 2 and 3 are presented together, comparing the results of “no control”, “ALINEA”, and “PI-ALINEA” in both cases, also in cross-comparison with Case 1. Extensive comparisons of ramp metering performance were conducted in different bottleneck cases using different controllers in order to address the following three questions:

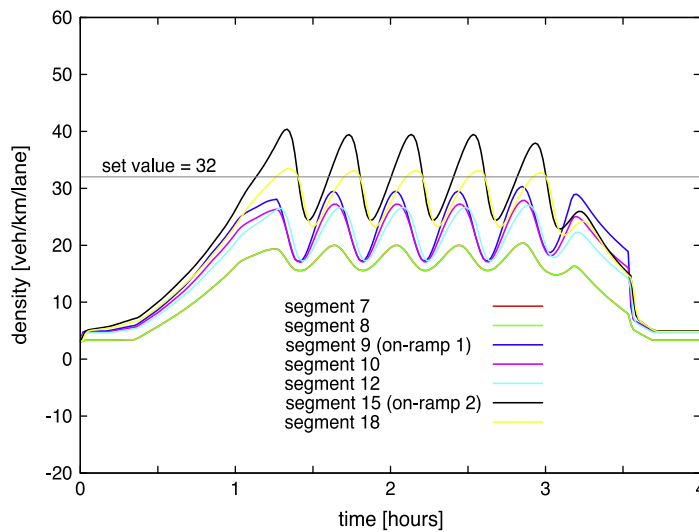
- (1) Does congestion of similar nature appear in each bottleneck case when the bottleneck is overloaded without ramp metering applied?
- (2) Does ALINEA perform well in any of the bottleneck cases, and does PI-ALINEA perform well in all cases?
- (3) Does ALINEA or PI-ALINEA, with an appropriately tuned parameter setting, have similar performance in all cases?

The ultimate intention is to demonstrate that PI-ALINEA operates similarly satisfactorily in all bottleneck cases, despite their substantial physical differences.

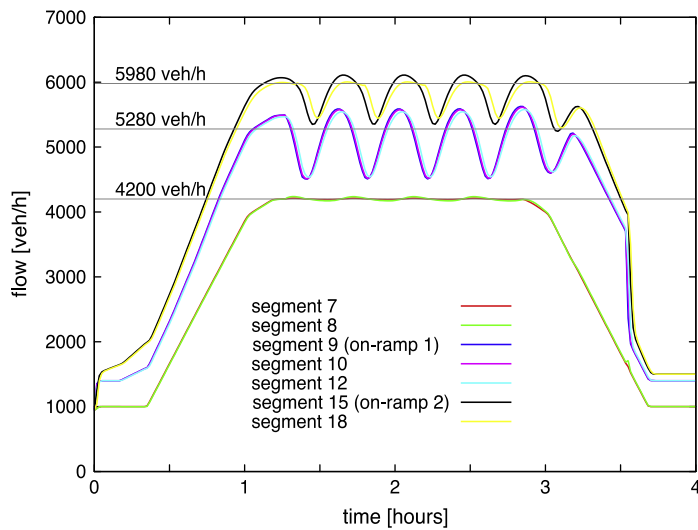
4.1. Bottleneck Case 1

4.1.1. No control

As previously mentioned, the factual maximum throughput (of 3 lanes) of the bottleneck in Bottleneck Case 1 is found to be 5270 veh/h. The total demand for the bottleneck (i.e. “mainstream demand” + “on-ramp demand” in Fig. 5a) during the peak period exceeds this capacity level. Therefore, in the case of no control, congestion occurs first in the bottleneck section (see the sudden rise of the black curve for segment 15 at 1.3 h in Fig. 6a), and spills back quickly to reach the on-ramp and



(a)



(b)

Fig. 11. ALINEA (Bottleneck Case 3, location 1): (a) segment densities; (b) segment flows.

gets intensified there while propagating further upstream (Fig. 6a). Congestion persists at the upstream of the bottleneck until the total demand decreases sufficiently. It is observed in the simulation that, during the whole peak period:

- (1) No segment downstream of the bottleneck gets congested due to the upstream-propagation of the shockwave (see e.g. the yellow curve in Fig. 6a for segment 18).
- (2) The outflows of the on-ramp segment and its downstream segments drop to around 5180 veh/h (<5270 veh/h) due to capacity drop incurred by congestion (Fig. 6b).
- (3) The peak-period throughput of all segments upstream of the on-ramp is the same (due to flow conservation) and lower than the mainstream demand (i.e. 3830 veh/h < 4400 veh/h, see Fig. 6b). In other words, the mainstream demand at the upstream of the on-ramp cannot be adequately served under congestion in the case of no-control.
- (4) The uncontrolled on-ramp inflow is equal to the on-ramp demand (1350 veh/h), which is exactly the observed flow difference between segments 9 and 8 in Fig. 6b

The above observations can be further explained as follows: Before the demand for the bottleneck rises up to the bottleneck capacity, the throughput of the bottleneck is equal to the arrival flow, see Fig. 6b for the period by 1 h. Once the demand rises above the bottleneck capacity, capacity drop is incurred and the capacity flow cannot be maintained. Specifically for the

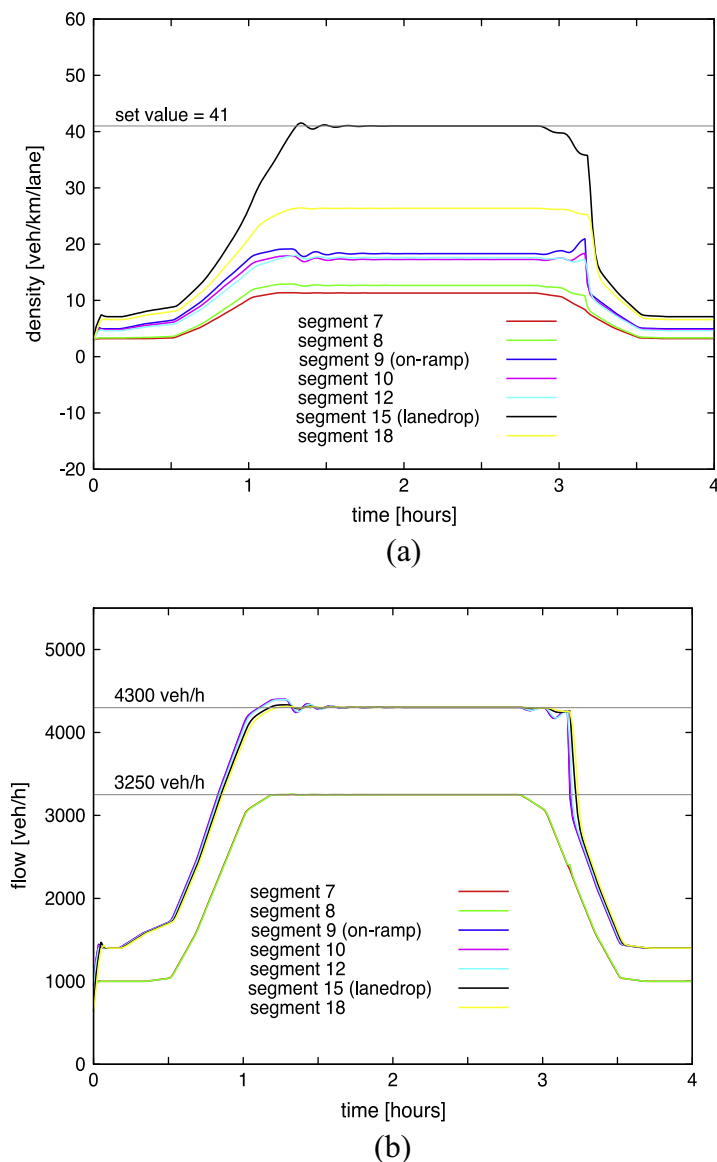
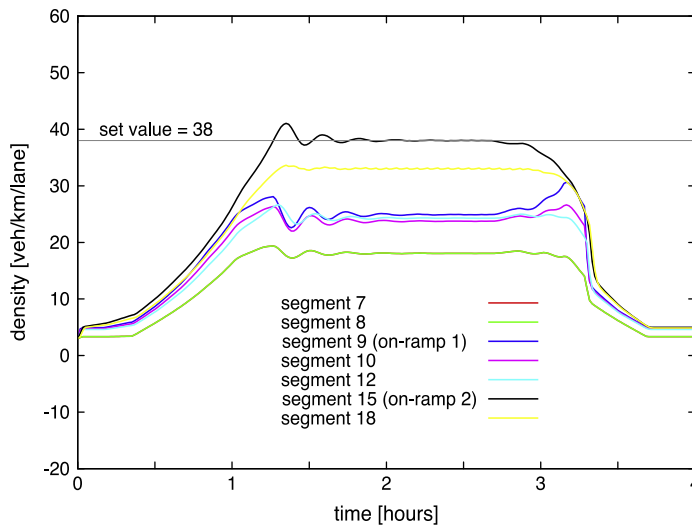


Fig. 12. PI-ALINEA (Bottleneck Case 2, location 1): (a) segment densities; (b) segment flows.

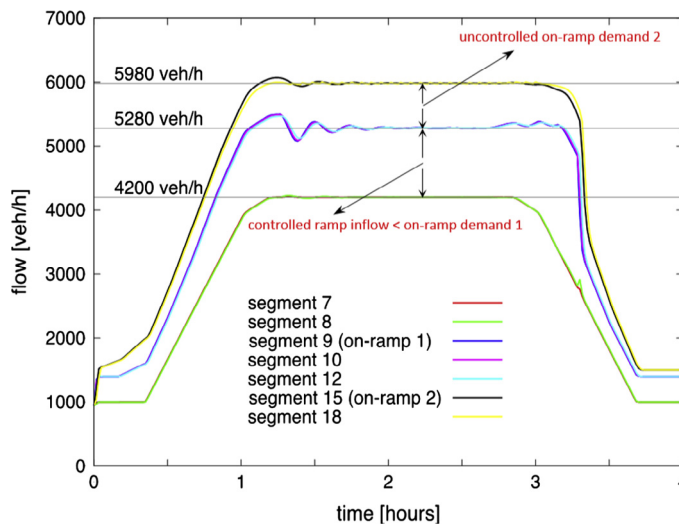
current simulation, the bottleneck flow drops from 5270 veh/h to 5180 veh/h, see segment 15 over the period (1 h, 2 h) in Fig. 6b. Before the congestion spills back to segments 9, its outflow during the peak period is equal to $4400 + 1350$ veh/h (Fig. 5a). When the congestion covers segment 9, its outflow is dominated by the bottleneck throughput 5180 veh/h, see segment 9 during the period (1 h, 2 h). For any further upstream segment (e.g. segment 8), before the congestion spills back to it, its outflow during the peak period is equal to 4400 veh/h (Fig. 5a). Once the congestion covers it, its outflow becomes equal to the bottleneck capacity minus the peak demand of the on-ramp, i.e. 3830 veh/h (Fig. 6b). In fact, the flow difference between left and right-hand side of the shockwave when the shockwave is within the stretch of segments 9–15 is $4400 + 1350 - 5180$ veh/h, and is $4400 - 3830$ veh/h when the shockwave reaches the upstream of segment 9.

4.1.2. ALINEA

The feedback ramp-metering controller ALINEA aims to keep the bottleneck flow around the bottleneck capacity so as to prevent congestion and capacity drop from occurring at the bottleneck. For this reason, ALINEA is fed with the density of segment 15. The ramp metering performance of ALINEA are presented in Fig. 7. The high-density profile is seen only in segment 15 and no other segment is ever congested (knowing that the factual critical densities of the bottleneck and



(a)



(b)

Fig. 13. PI-ALINEA (Bottleneck Case 3, location 1): (a) segment densities; (b) segment flows.

regular segments are 42 veh/km and 38 veh/km). Though the congestion spillback is prevented, the resulting density profiles of segment 15 and the neighboring segments are strongly oscillating. In the meantime, the average throughput downstream of the on-ramp is lower than the bottleneck capacity (5270 veh/h), which is anyhow sufficient to serve the mainstream demand (4400 veh/h), in contrast to the no control case (Fig. 6b vs. Fig. 7b). Note that the presented ALINEA results are the best possible results for this test example, out of a trade-off between the density/flow oscillation amplitude and the mean bottleneck throughput. To obtain these results, the parameter K_R of ALINEA was reduced to 10 km-lane/h from its original/standard value of 40 km-lane/h (Papageorgiou et al., 1991; Wang et al., 2014). Using the standard K_R value, however, ALINEA can produce a higher bottleneck outflow (still lower than its capacity), which is however at the cost of much stronger oscillation in the density and flow profiles than seen with Fig. 7. Apparently, ALINEA in this bottleneck case is only OK in serving the mainstream demand but not capable of maintaining the bottleneck capacity flow. The observed oscillatory behavior is due to the significant distance or time delay between the ramp flow change and its impact on the traffic flow dynamics at the downstream bottleneck (Wang et al., 2014). As an I-regulator, ALINEA is known to have difficulties in dealing with such time delay, while PI-ALINEA, as a PI-regulator, can satisfactorily handle time delays (with appropriate parameter values).

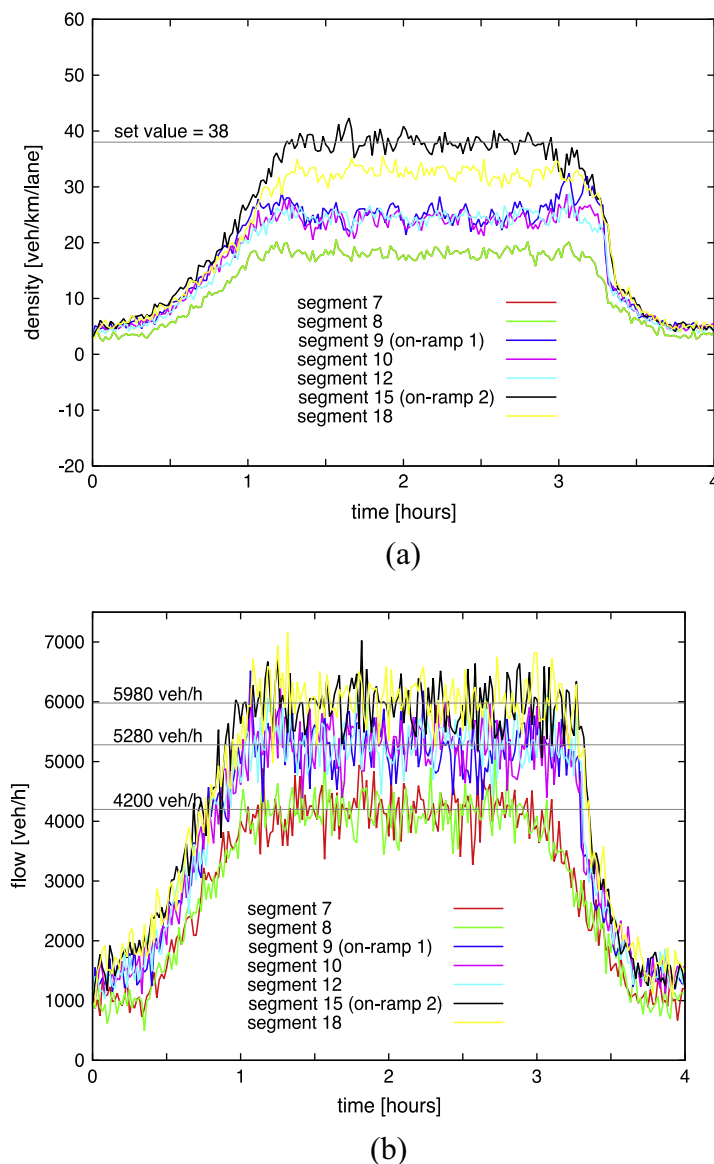


Fig. 14. PI-ALINEA (Bottleneck Case 3, location 1, stochastic): (a) segment densities; (b) segment flows.

4.1.3. PI-ALINEA

In striking contrast, the ramp metering results with PI-ALINEA using the same measurements are very satisfactory (Fig. 8). The response trajectory of the density in segment 15 is very smooth, only with a short transient period and a small overshoot. In the steady state, the density of segment 15 is kept exactly at the set value, while the capacity level of the bottleneck section is achieved and the mainstream demand is well served. Except for segment 15, where the critical density prevails, all other segments are in free-flow conditions. The utilized K_R and K_p parameters were set to 4 km·lane/h and 100 km·lane/h, respectively, but, moderately different values were found to have little impact on the quality of the control results (Kotsialos et al., 2006). Obviously, the time-delay effect in the ALINEA case is well treated by use of PI-ALINEA. PI-ALINEA was also tested with a more realistic stochastic scenario, whereby the traffic demand is involved with noise and the model equations include appropriate stochastic terms (see Wang and Papageorgiou, 2005 for the details). Again, the density of segment 15 in this case is kept around the set value (Fig. 9a) and the bottleneck throughput is around capacity (Fig. 9b).

4.2. Bottleneck Cases 2 and 3

Simulation studies on the performance of ALINEA and PI-ALINEA are also conducted with respect to Bottleneck Cases 2 and 3. Without ramp metering applied, the density and flow profiles in Bottleneck Case 2 are quite similar to those in Case 1. The results from Case 3 are displayed in Fig. 10. The detailed analysis made for Case 1 (Section 4.1.1) also applies to the Cases 2 and 3.

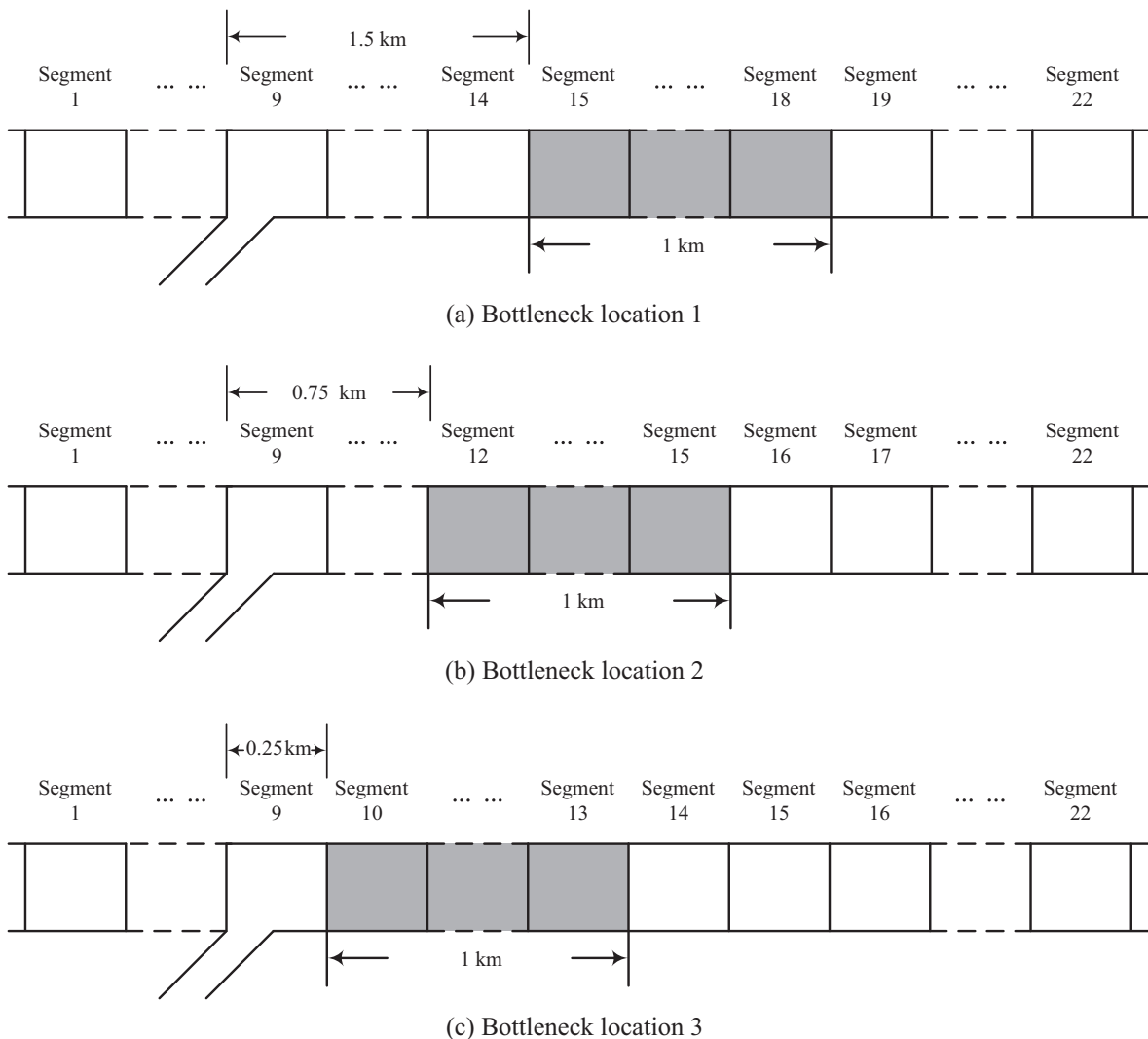


Fig. 15. A freeway stretch with a downstream bottleneck at different locations.

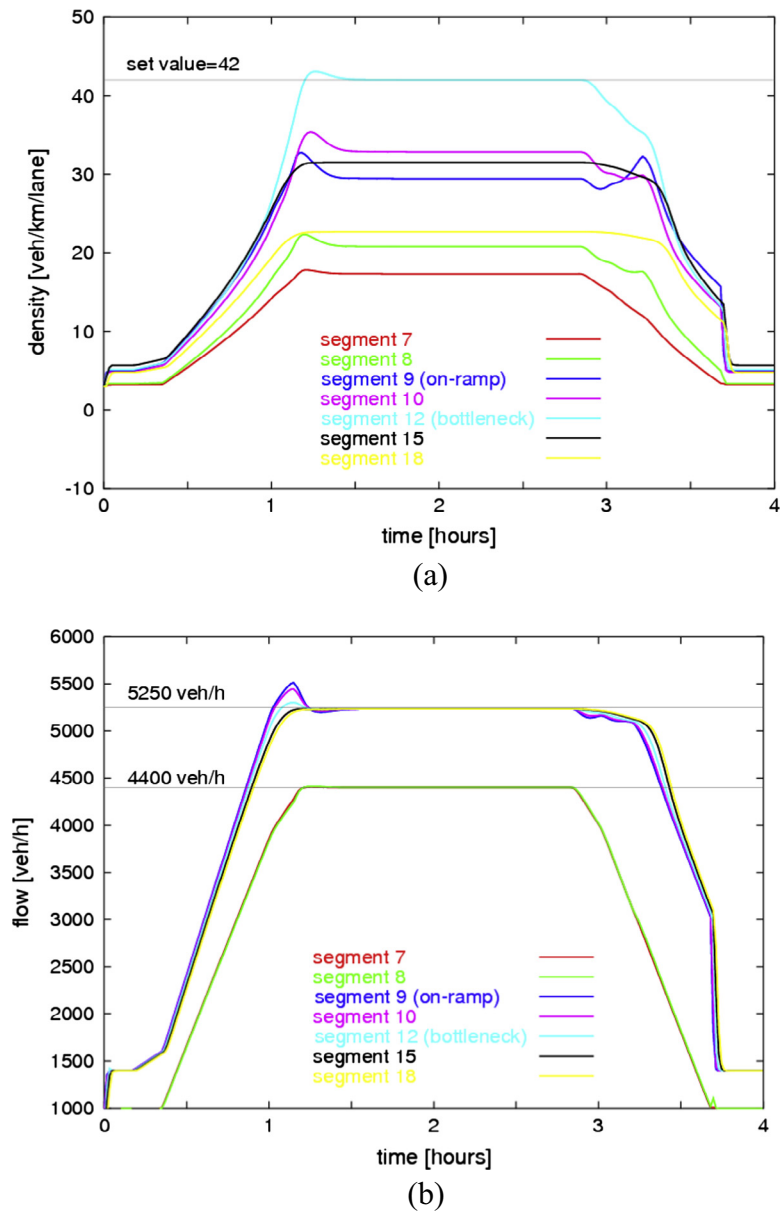
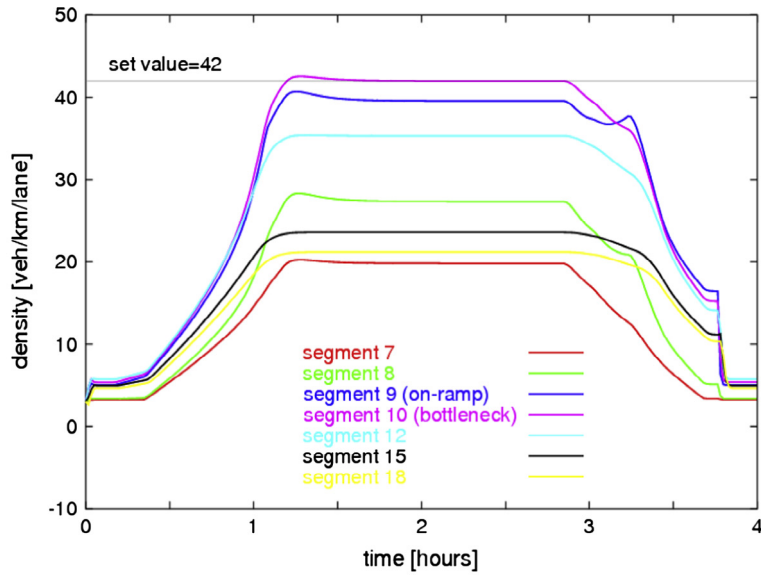


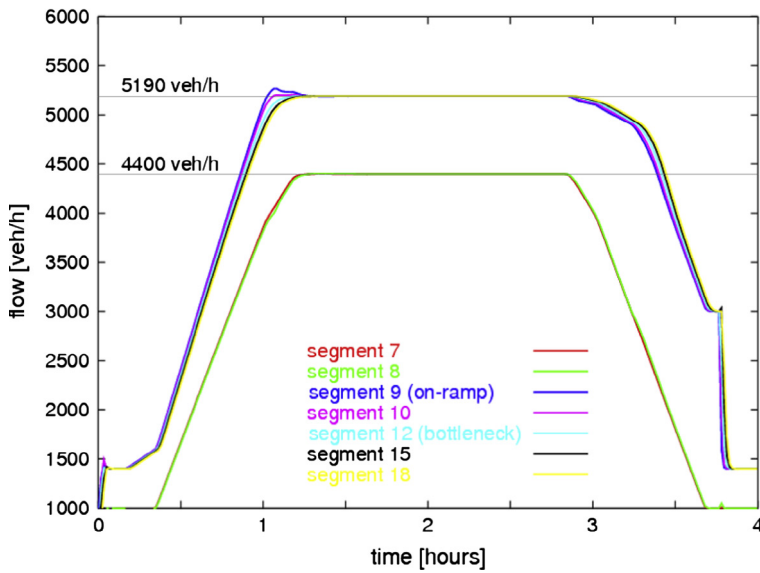
Fig. 16. PI-ALINEA (Bottleneck Case 1, location 2): (a) segment densities; (b) segment flows.

In spite of different mechanisms in creating the bottlenecks, ALINEA delivers very similar results (at large) in three cases; see Fig. 11 for the results in the case of Bottleneck 3, in comparison to Fig. 7 for Bottleneck Case 1. Note that the same K_R parameter of ALINEA is used for the three bottleneck cases. Though ALINEA can manage to get the upstream demand toward segment 9 well served in each case, it can neither stabilize the density in the segment 15 (the target segment) nor maximize the flow throughput there.

On the other hand, very consistent results are obtained with PI-ALINEA in the three bottleneck cases (see Figs. 8, 12 and 13). For Case 3, the flow in segment 15 is maximized to be around the mainstream capacity of 6000 veh/h (Fig. 13b), despite the unknown and uncontrolled on-ramp demand at segment 15. Thus, the flow difference between Segments 12 and 15 is actually the un-controlled demand of the second on-ramp while that between segments 8 and 9 is actually the controlled inflow at the first on-ramp. The stochastic effect was also considered, and as an example, the PI-ALINEA performance for Bottleneck 3 is presented in Fig. 14a and b. It should be emphasized that all PI-ALINEA results were obtained with the same K_R and K_P parameters ($K_R = 4$ km-lane/h and $K_P = 100$ km-lane/h). This once more indicates the general applicability of PI-ALINEA in the case of a far downstream bottleneck.



(a)



(b)

Fig. 17. PI-ALINEA (Bottleneck Case 1, location 3): (a) segment densities; (b) segment flows.

4.3. The bottleneck locations

So far, a fixed bottleneck location (segment 15) has been considered for each bottleneck case (Fig. 3). To test the sensitivity of ALINEA and PI-ALINEA (of the same parameterization) as to the distance between the bottleneck and on-ramp, two more bottleneck locations are also considered for each bottleneck case, see Fig. 15 for an illustration. The demand profiles are identical with those previously considered. The PI-ALINEA results with respect to the 2nd and 3rd bottleneck locations in Bottleneck Case 1 are presented in Figs. 16 and 17. The PI-ALINEA results with respect to the 2nd bottleneck location in Bottleneck Cases 2 and 3 are presented in Fig. 18a and b. Apparently, these PI-ALINEA results are quite similar to those in Figs. 8, 12a, and 13a, albeit with better damping.

The ALINEA results for Bottleneck Case 1 at Locations 2 and 3 are presented in Figs. 19a and b. The comparison of Figs. 7a, 19a and b indicates that, the closer the bottleneck to the on-ramp, the better ALINEA results. In the limit case, when

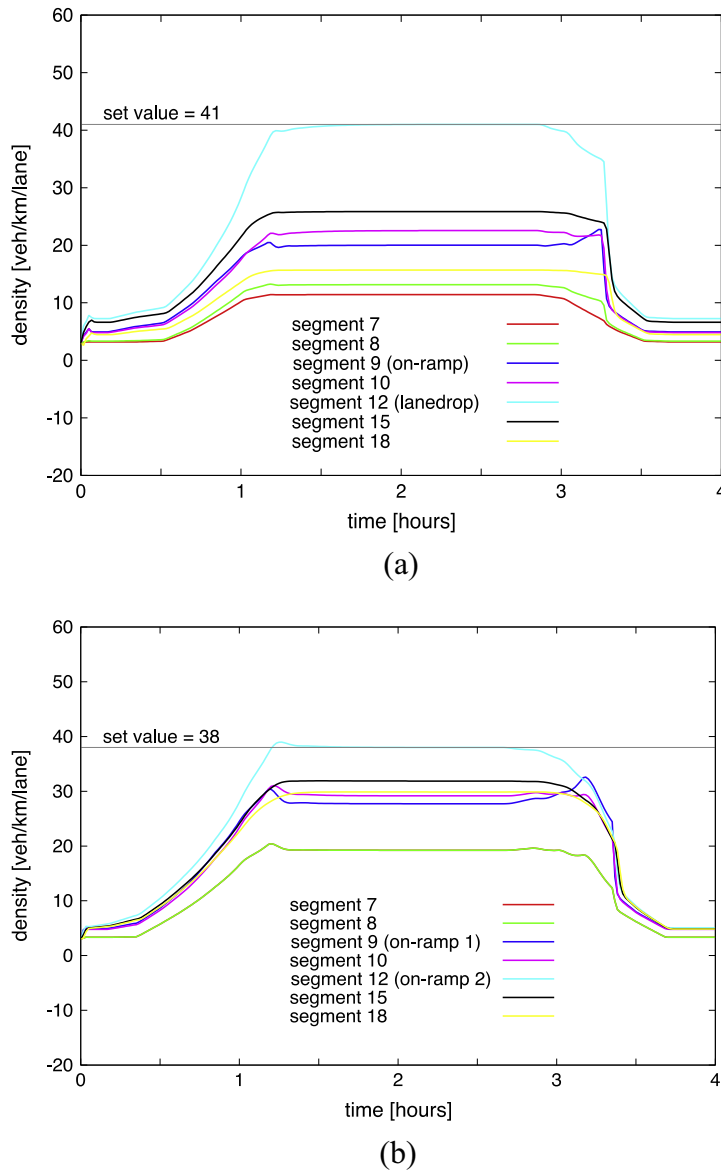


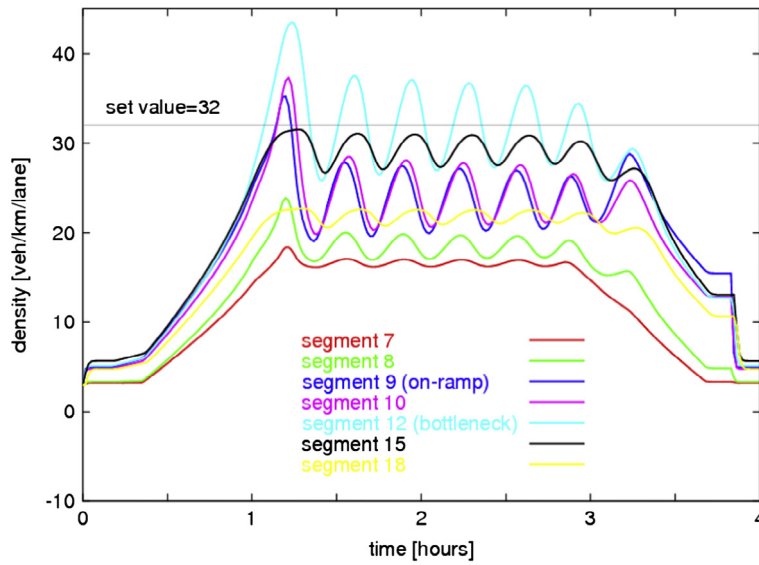
Fig. 18. PI-ALINEA (location 2): (a) Bottleneck case 2; (b) Bottleneck case 3.

the bottleneck is exactly located in the merging area, in which case there is no so-called downstream bottleneck and the merging segment 9 essentially plays the role of a bottleneck, satisfactory ALINEA results are obtained.³ ALINEA at the 2nd and 3rd locations in the other two bottleneck cases deliver no surprising results. In summary, ALINEA is getting less damped and more oscillatory with the increasing distance between the on-ramp and the downstream bottleneck, which is consistent with the theoretical expectation (Wang et al., 2014). In contrast, PI-ALINEA is little sensitive to this distance.

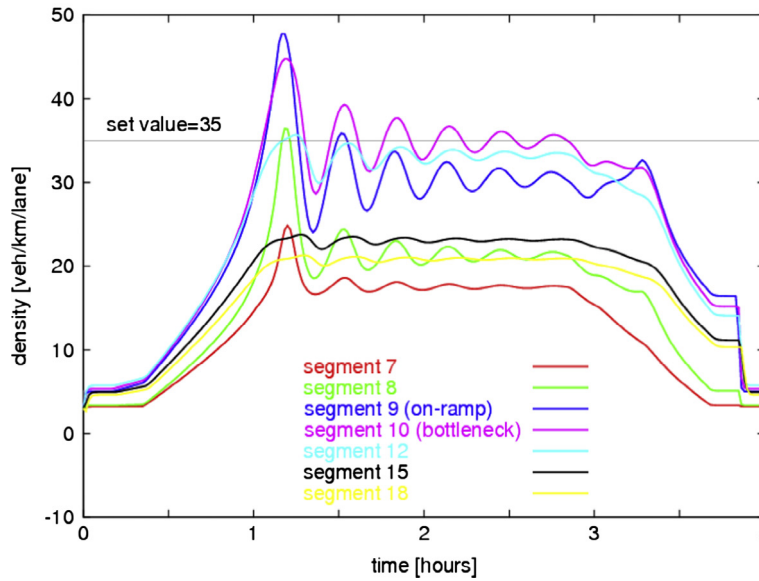
5. A field application example

In early 2008, via a pilot project funded by VicRoads, the Victorian transport authority in Australia, the heuristic ramp-metering coordination (HERO) strategy (Papamichail et al., 2010) was implemented and became operational at six consecutive inbound on-ramps along a 20-km stretch of the Monash Freeway in Melbourne, Australia. The test stretch extends from Jacksons Road to Warrigal Road, as shown in Fig. 20. HERO includes and coordinates local ALINEA or PI-ALINEA regulators, which are

³ By its design philosophy, ALINEA is doomed to work well in this case (Wang et al., 2014).



(a)



(b)

Fig. 19. ALINEA (Bottleneck Case 1): (a) location 2; (b) location 3.

employed independently at each ramp to address the respective (potential) bottlenecks. With HERO via this pilot project, PI-ALINEA was actually tested for the first time in field operation, but the test results were not specifically reported before. We present here some of the obtained results with respect to a bottleneck located about 2.8 km downstream of the Warrigal Road merge area (Fig. 20).

The bottleneck was activated during the morning peak period every day due to strong weaving around that location. As a result, the bottleneck capacity was lower than the merge area capacity of the Warrigal Road on-ramp; hence, PI-ALINEA was employed at the on-ramp to address this distant downstream bottleneck, using occupancy measurements from the bottleneck. At the time of this project, Monash Freeway was a 3-lane freeway, and the critical occupancy in the bottleneck area was found to be equal to 22%. The application of PI-ALINEA during the morning peak was successful in maintaining the downstream bottleneck occupancy around the corresponding critical occupancy, thus maximizing the bottleneck throughput. Fig. 21 displays a typical sample of the controlled bottleneck occupancy, where it may be seen that the occupancy is stabi-

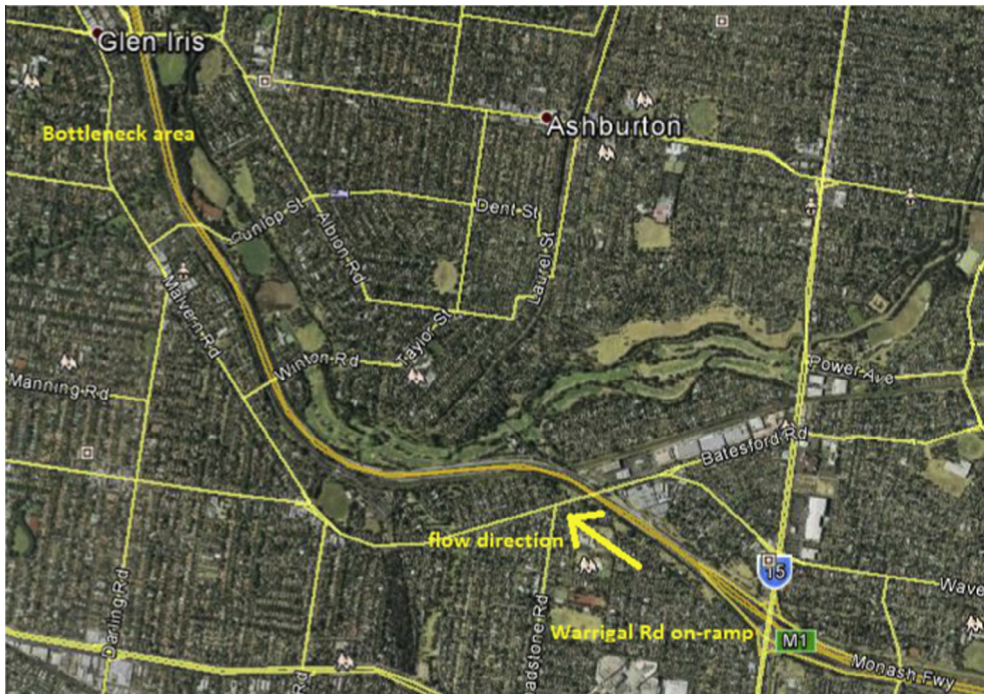


Fig. 20. The area map of the Monash Freeway with Warrigal Rd on-ramp and its far-downstream bottleneck.

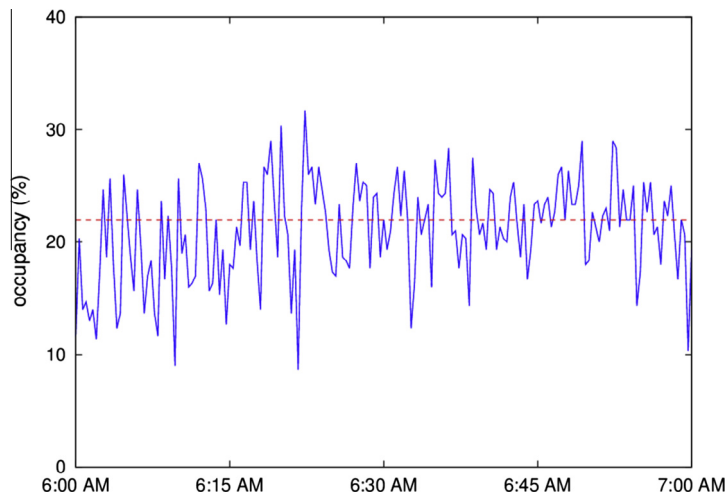


Fig. 21. Occupancy measurements and the PI-ALINEA set-value at the bottleneck location.

lized around the set value as long as the freeway demand for the bottleneck is sufficiently high (after 6:15 AM). Fig. 22 displays the flow achieved at the bottleneck for the same period; while Fig. 23 displays the estimated on-ramp queue (Vigos et al., 2008). It can be observed that, after 6:15 AM, capacity flow is achieved (6000–6100 veh/h in average) thanks to the ramp metering operation with PI-ALINEA; this entails the creation of a ramp queue after 6:15 AM, since the ramp demand exceeds (in average) the ramp flow requested by PI-ALINEA. Quantitatively, the PI-ALINEA parameters that led to the above results were found to be very close to those used for the simulations studies.

6. Conclusions

The reported simulation studies demonstrate that ALINEA behaves in a low-damped manner and is not capable of maintaining the maximum throughput in the presence of a distant downstream bottleneck of any type. On the other hand,

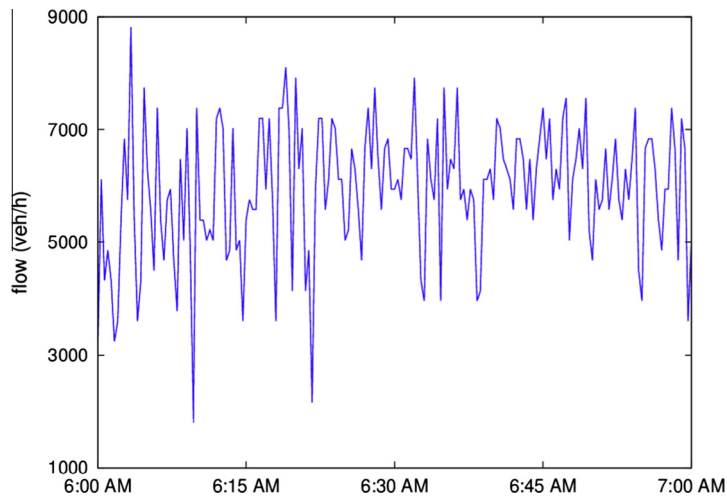


Fig. 22. Flow measurements at the bottleneck location.

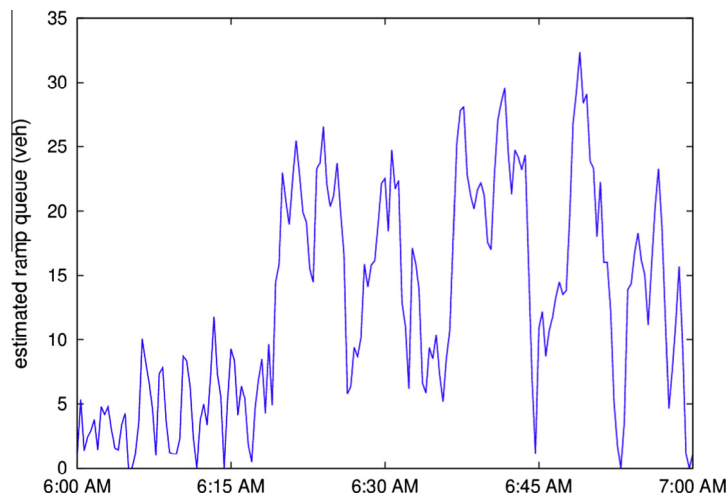


Fig. 23. The estimated vehicle queue at the Warrigal Road on-ramp.

PI-ALINEA is universally efficient in handling the local ramp-metering task in such bottleneck cases. In addition, little fine-tuning of the regulator is necessary, because consistent parameterization of PI-ALINEA applies in various circumstances of bottleneck type and location as well as for field applications. It should be stressed that the proposed PI-ALINEA structure is currently only applicable if the downstream bottleneck location is known beforehand so as to have traffic sensors deployed there. In addition, it should not be forgotten that, without a typical downstream bottleneck as addressed in this paper, ALINEA and PI-ALINEA work equally well in handling ramp metering (Wang et al., 2014).

Acknowledgements

The research reported in this paper was supported in part by the Zhejiang Qianren Program (2013–2018), the National Natural Science Foundation of China (Project number: 51478428), and the European Research Council under the European Union's Seventh Framework Programme (FP/2007-2013)/ERC Grant Agreement No. 321132, project TRAMAN21.

References

- Bhouri, N., Haj-Salem, H., Kauppila, J., 2013. Isolated versus coordinated ramp metering: field evaluation results of travel time reliability and traffic impact. *Transp. Res. Part C* 28, 155–167.
- Frejo, J.R.D., Camacho, E.F., 2012. Global versus local MPC algorithms in freeway traffic control with ramp metering and variable speed limits. *IEEE Trans. Intell. Transp. Syst.* 13 (4), 1556–1565.

- Geroliminis, N., Srivastava, A., Michalopoulos, P., 2011. A dynamic-zone-based coordinated ramp-metering algorithm with queue constraints for Minnesota's freeways. *IEEE Trans. Intell. Transp. Syst.* 12 (4), 1576–1586.
- Gomes, G., Horowitz, R., 2006. Optimal freeway ramp metering using the asymmetric cell transmission model. *Transp. Res. Part C* 14 (4), 244–262.
- Hegyi, A., De Schutter, B., Hellendoorn, H., 2005. Model predictive control for optimal coordination of ramp metering and variable speed limits. *Transp. Res. Part C* 13 (3), 185–209.
- Kotsialos, A., Kosmatopoulos, E., Manolis, D., Papageorgiou, M., Vigos, G., Wang, Y., et al., 2006. Simulation testing for local ramp metering strategies. Deliverable D3.2 for the Project EURAMP (IST-2002-23110), Report for the Information Society Technologies Office of the European Commission, Brussels, Belgium.
- Li, Y., Chow, A.H.F., Cassel, D.L., 2014a. Optimal control of motorways by ramp metering, variable speed limits, and hard-shoulder running. *Transp. Res. Rec.* 2470, 122–130.
- Li, D., Ranjitkar, P., Ceder, A., 2014b. Integrated approach combining ramp metering and variable speed limits to improve motorway performance. Paper Presented at the Transportation Research Board 93rd Annual Meeting, no. 14-3781.
- Lu, X.Y., Varaiya, P., Horowitz, R., Su, D.Y., Shladover, S.E., 2011. Novel freeway traffic control with variable speed limit and coordinated ramp metering. *Transp. Res. Rec.* 2229, 55–65.
- Meng, Q., Khoo, H.L., 2010. A Pareto-optimization approach for a fair ramp metering. *Transp. Res. Part C* 18 (4), 489–506.
- Papageorgiou, M., Kotsialos, A., 2002. Freeway ramp metering: an overview. *IEEE Trans. Intell. Transport. Syst.* 3, 271–281.
- Papageorgiou, M., Blosseville, J.-M., Haj-Salem, H., 1990. Modelling and real-time control of traffic flow on the southern part of Boulevard Périphérique in Paris – Part I: Modelling. *Transp. Res. Part A* 24, 345–359.
- Papageorgiou, M., Hadj-Salem, H., Blosseville, J.-M., 1991. ALINEA: a local feedback control law for on-ramp metering. *Transp. Res. Rec.* 1320, 58–64.
- Papamichail, I., Papageorgiou, M., 2008. Traffic-responsive linked ramp-metering control. *IEEE Trans. Intell. Transport. Syst.* 9, 111–121.
- Papamichail, I., Papageorgiou, M., Vong, V., Gaffney, J., 2010. Heuristic ramp-metering coordination strategy implemented at Monash Freeway. *Transport. Res. Record: J. Transport. Res. Board* 2178, 10–20.
- Vigos, G., Papageorgiou, M., Wang, Y., 2008. Real-time estimation of vehicle-count within signalized links. *Transp. Res. Part C* 16, 18–35.
- Wang, Y., Papageorgiou, M., 2005. Real-time freeway traffic state estimation based on extended Kalman filter: a general approach. *Transp. Res. Part B* 39, 141–167.
- Wang, Y., Kosmatopoulos, E., Papageorgiou, M., Papamichail, I., 2014. Local ramp metering in the presence of a distant downstream bottleneck: theoretical analysis and simulation study. *IEEE Trans. Intell. Transport. Syst.* 15 (5), 2024–2039.